

RESEARCH

Open Access



LINC00968 accelerates osteogenic differentiation of bone marrow mesenchymal stem cells via the miR-17-5p/STAT3 axis

Shanglong Ning¹, Yang Chen¹ and Hui Zhu^{2*}

Abstract

Background BMSCs with robust osteogenic differentiation capacity can participate in the repair of osteoporotic (OP) bone. Long non-coding RNAs (LncRNAs) serve as crucial regulators of osteogenic differentiation. This study aims to investigate the clinical implications of LINC00968 in OP and elucidate its molecular mechanisms.

Methods Patients with OP and controls without OP were enrolled. RT-qPCR was utilized to quantify the levels of LINC00968, miR-17-5p, STAT3, and osteogenic differentiation markers. ROC curve was conducted to evaluate the diagnostic significance. Osteogenic differentiation medium (OM) induced hBMSCs. Flow cytometry was used to examine apoptosis. DLR and RIP assay were performed to validate target binding.

Results LINC00968 was notably decreased in the serum and bone tissue of patients with OP, whereas it was markedly elevated during osteogenic differentiation of hBMSCs. LINC00968 has 78.65% sensitivity and 71.95% specificity in identifying OP patients from controls. Silencing of LINC00968 sharply diminished ALP activity and osteogenic differentiation markers levels while promoting apoptosis in hBMSCs under OM induction. However, this reduction was notably reversed by the administration of a miR-17-5p inhibitor. Molecularly, miR-17-5p directly targets LINC00968 and STAT3.

Conclusions Our results indicate that LINC00968 downregulation is a diagnostic biomarker for OP, facilitating osteogenic differentiation and inhibiting apoptosis via miR-17-5p/STAT3 axis, suggesting a new therapeutic target for OP progression.

Keywords Osteoporotic, LINC00968, Osteogenic differentiation, miR-17-5p, STAT3

*Correspondence:

Hui Zhu
zhuhui840626@163.com

¹Department of Spine Surgery, Tianjin Hospital, Tianjin University,
Tianjin 300211, China

²Department of Radiation Oncology, Tianjin Medical University Cancer
Institute and Hospital, National Clinical Research Center for Cancer, No.1,
Huanhu West Road, North Sports Institute Road, Hexi District,
Tianjin 300000, China



© The Author(s) 2025. **Open Access** This article is licensed under a Creative Commons Attribution-NonCommercial-NoDerivatives 4.0 International License, which permits any non-commercial use, sharing, distribution and reproduction in any medium or format, as long as you give appropriate credit to the original author(s) and the source, provide a link to the Creative Commons licence, and indicate if you modified the licensed material. You do not have permission under this licence to share adapted material derived from this article or parts of it. The images or other third party material in this article are included in the article's Creative Commons licence, unless indicated otherwise in a credit line to the material. If material is not included in the article's Creative Commons licence and your intended use is not permitted by statutory regulation or exceeds the permitted use, you will need to obtain permission directly from the copyright holder. To view a copy of this licence, visit <http://creativecommons.org/licenses/by-nc-nd/4.0/>.

Background

Osteoporosis (OP) is a chronic and disabling disease characterized by reduced bone mass, deterioration of bone microarchitecture, and a high risk of fragility fractures [1]. Globally, over 200 million individuals are affected by OP, with a prevalence rate of more than 25%, ranking 6th among common and prevalent diseases [2]. OP-induced fractures and complications pose serious risks of disability and death among the elderly. However, OP is often asymptomatic in its early stages, resulting in patients typically being diagnosed only when they suffer a low-energy fracture. This, in turn, leads to the neglect of effective fracture management and prevention strategies [3]. Early detection and intervention in OP are critical to preventing fragility fractures and slowing disease progression. Bone marrow mesenchymal stem cells (BMSCs) function as osteoblast progenitor cells and serve as crucial factors in the formation of new bone tissues. Imbalanced osteogenic and adipocyte differentiation of BMSCs can underlie the pathogenesis of OP. However, the mechanisms underlying the induction and enhancement of osteogenic differentiation in BMSCs remain an area of active and in-depth research.

Long non-coding RNAs (LncRNAs), which constitute a class of RNA transcripts that do not encode proteins, play roles in a variety of pathophysiological processes due to their abundance and potential dysregulation. For instance, lncRNA H19 [4], lncTIMP3 [5], and IGF2-AS [6] have been implicated in the osteogenic differentiation of BMSCs. Long intergenic non-protein coding RNA 968 (LINC00968), a novel lncRNA, is located on human chromosome 8q12.1. Previous studies have discovered that LINC00968 promotes the progression of osteosarcoma as an oncogene [7]. Strikingly, Liao et al. (2020) reported that LINC00968 promotes mineralized bone matrix, alkaline phosphatase (ALP) activity, and the levels of osteogenic markers in dental pulp stem cells and is a novel target for maxillary posterior dental implants [8]. LINC00968 has also been associated with osteogenic differentiation of dental pulp stem cells and zebrafish scale regeneration [9]. Of note, Qiu et al. (2017) conducted a microarray analysis to identify abnormally expressed lncRNAs during osteogenic differentiation of human BMSCs (hBMSCs), highlighting LINC00968 as one of the lncRNAs with a significant fold change greater than 2 [10]. While the involvement of LINC00968 in osteogenic differentiation of dental pulp stem cells has been reported, however, the role of LINC00968 in OP, a specific pathological condition, is a completely new area of research and is a specific mechanism of action, regulatory network, and potential clinical application value are still unclear.

MicroRNAs (miRNAs) are short, single-stranded non-coding RNAs that participate in the regulation of

musculoskeletal system functions by binding to target mRNAs [11–15]. Previous studies show that miR-17-5p reduces bone mineral density [16] and is higher in postmenopausal OP patients [17]. miR-17-5p targeting signal transducer and activator of transcription 3 (STAT3) in rheumatoid arthritis (19), bladder cancer (28), and myocardial ischemia-reperfusion injury (29) has been reported. STAT3, a STAT family member, is crucial for skeletal development and bone repair [18]. It's a key target for slowing OP progression, with catalpol [19] and naringenin [20] both showing effectiveness. STAT3 levels rise significantly in osteogenic differentiation of hBMSCs [21]. Whether miR-17-5p alleviates OP by targeting STAT3 is unclear. It is well known that lncRNA can function as ceRNA sponging miRNA and upregulate the mRNA. Bioinformatics predicts LINC00968 binds miR-17-5p, but whether LINC00968 affects OP by regulating miR-17-5p/STAT3 needs further study.

Here, we hypothesize that LINC00968 could alleviate the progression of OP by targeting miR-17-5p/STAT3 to regulate the osteogenic differentiation of BMSCs. To test our hypothesis, we analyzed the levels of LINC00968 in patients with OP and investigated its mechanism of action in regulating the differentiation of BMSCs in an *in vitro* study. Our objective was to gain a deeper understanding of novel mechanisms that could potentially alleviate OP. By doing so, we aim to fill the knowledge gap regarding the role of LINC00968 in modulating the differentiation of BMSCs and its potential therapeutic implications in OP.

Methods

Clinical samples

The study was approved by the Tianjin Hospital Research Ethics Committee (Approval number: 2022-098). The experimental procedures were under the standards fixed in the Declaration of Helsinki, and the subjects were informed about the research design and signed an informed consent form. 89 patients with OP (51 females, 66.76 ± 9.10 years) who underwent hip arthroplasty for femoral neck fracture were included. Additionally, 82 patients with non-osteoporotic fracture due to traumatic fracture (44 females and 68.98 ± 9.73 years) and age and gender-matched OP patients were included as controls. Patients in both groups did not receive any medication before treatment and were excluded from rheumatoid arthritis, cancer, diabetes mellitus hyperthyroidism, hyperparathyroidism, and nephropathy. Trabecular bone tissue samples were obtained from the femoral trochanter area away from the periarticular bone during the study. Meanwhile, 5 ml of peripheral venous blood was collected and then centrifuged at $3000 \times g$ for 5 min to collect serum samples.

Cell culture and osteogenic induction

hBMSCs were derived from the American Type Culture Collection (ATCC; Catalog no. PCS-500-012) and cultured in DMEM proliferation medium (PM, catalog no. SH30022.01B, Hyclone) containing 10% fetal bovine serum (FBS, catalog no. A2720801, Gibco) and maintained in an incubator at 37°C with 5% CO₂. To identify hBMSCs, cells from passage 3 were digested and subjected to flow cytometry. After washing with pre-cooled PBS for resuspension, 1 × 10⁵ cells were stained with antibodies specific to CD29 (catalog no. 11-0299-42), CD44 (catalog no. 11-0441-82), CD73 (catalog no. 11-0739-42), CD105 (catalog no. MAL-19594), and CD45 (catalog no. 11-0459-42, Thermo Fisher Scientific) under light-protected conditions for 30 min. Subsequently, the stained cells were analyzed using a flow cytometer.

For induction of osteogenic differentiation, hBMSCs were placed in osteogenic differentiation medium (OM) supplemented with 0.05 mmol/L ascorbic acid (catalog no. A5960, Sigma), 100 mmol/L dexamethasone, and 10 mmol/L β-glycerophosphate (catalog no. G9891, Sigma-Aldrich). The OM medium was changed every 3 days and cells were collected after 0, 3, 7, and 14 d of differentiation.

Cell transfection

The small interfering RNA targeting LINC00968 (si-LINC00968) and negative control (si-NC) were obtained from GenePharma. miR-17-5p inhibitor (catalog no. miR20000786-1-5) and inhibitor NC (catalog no. miR2N0000001-1-5) were purchased from RiboBio. hBMSCs were plated at a density of 4 × 10⁵ cells/well in 6-well plates, and transferred with 80 nM si-LINC00968, si-NC, or 50 nM miR-17-5p inhibitor or inhibitor NC using 5 μL Lipofectamine 2000 (catalog no. 11668-019, Life Technologies) during the logarithmic growth phase (60–80% confluence). 6 h later, the medium was changed to OM medium for 3 consecutive days. The transfection efficiency was then assessed using reverse transcription quantitative chain reaction (RT-qPCR) assays.

RNA extraction and reverse transcription-quantitative reverse transcription PCR (RT-qPCR)

RNA was extracted from serum samples and hBMSCs using a TRIzol reagent (catalog no. 15596026, Thermo Fisher Scientific). The purity and quantity of RNA were verified using a NanoDrop technology (NanoDrop 2000c spectrophotometer, Thermo Scientific). Subsequently, 1 μg of total RNA was reverse transcribed into complementary DNA (cDNA) using the primer-Script RT reagent kit (catalog no. RR037A, Takara). A mixture of cDNA, primers, H₂O, and SYBR R Premix Ex Taq™ II kit (catalog no. RR802A, Takara) was prepared, and the amplification reaction was conducted on the CFX96 Touch System

(Bio-Bad). The relative expression of LINC00968, osteopontin (OPN), osteocalcin (OCN), and runt-related transcription factor 2 (RUNX2) was normalized to GAPDH. miR-17-5p expression was quantitatively assessed using the TaqMan MiRNA Reverse Transcription Kit (catalog no. 4366597, Applied Biosystems) followed by RT-qPCR reactions with the TaqMan Human MiRNA Assay Kit (catalog no. 4427975, Applied Biosystems), normalizing to U6 snRNA. Calculations of relative gene expression were performed using the 2^{-ΔΔCt} method, with three biological and two technical replicates for each biological sample. Primer sequences used were listed as follows: LINC00968 forward, 5'-GCCCAGTTGACAGGAAATG T-3'; and reverse 5'-TTGGTTCTCAATGGGATGGT-3'; OPN forward, 5'-GATGAATCTGATGAACTGGTCA CT-3'; and reverse 5'-GGTGATGTCCTCGTCTGTAG CA-3'; ONC forward, 5'-GACGAGTTGGCTGACCAC A-3'; and reverse 5'-CAAGGGGAAGAGGAAAGAAG G-3'; RUNX2 forward, 5'-TAGGCGCATTTCAGGTG CTT-3'; and reverse 5'-GGTGTGGTAGTGAGTGGTG G-3'; GAPDH forward, 5'-GGAGCGAGATCCCCTCAA AAT-3'; and reverse 5'-GGCTCTTGTCATACTTCTCAT GG-3'; miR-17-5p forward, 5'-ACACTCCAGCTGGGC AAAGTGCTTACAGTGC-3'; and reverse 5'-CTCAACT GGTGTCGTGGA-3'; U6 forward, 5'-CTCGCTTCGGC AGCACA-3'; and reverse 5'-AACGCTTACGAATTTG CGT-3'. RT-qPCR was performed at 95°C for 2 min, followed by 40 cycles of 95°C for 5 s and 60°C for 30 s.

Western blotting assay

Total protein was extracted from transfected 72 h and OM-induced hBMSCs by adding RIPA lysis buffer (catalog no. P0013B, Beyotime) containing protease/phosphatase inhibitor cocktail (catalog no. 5872, Cell Signaling Technology). Total protein was quantified by a BCA protein assay kit (catalog no. P0012S, Beyotime). 25 μg of total protein was added to the wells of the SDS-PAGE gel and electrophoresed at 120 mA for 90 min, after which the proteins were transferred to a PVDF membrane (catalog no. FFP24, Beyotime). 5% bovine serum albumin (catalog no. A7906, Sigma-Aldrich) was incubated for 2 h at room temperature. The primary antibodies anti-osteocalcin (1:1000; catalog no. ab93876, Abcam), anti-osteopontin (1:1000; catalog no. ab8488, Abcam), anti-RUNX2 (1:1000; catalog no. ab76956, Abcam), anti-GAPDH (1:2500; catalog no. ab9485, Abcam) were incubated with PVDF membrane at 4°C for 12 h, respectively. The PVDF membrane was subsequently incubated with HRP-conjugated goat anti-rabbit IgG (1:3000; catalog no. ab6721; Abcam) for 2 h at room temperature. The protein bands were then observed using a Tanon-5200 chemical discharge image (Tanon Science and Technology), and the band density was quantitatively analyzed using Image

J software (version 1.52q, National Institutes of Health, Bethesda).

Cell apoptosis assay

Apoptosis was detected using Annexin V-fluorescein isothiocyanate (FITC)/propidium iodide (PI) double staining kit (catalog no. 556547, BD biosciences) and flow cytometry. Briefly, cells transfected for 72 h and OM-induced for 0, 3, 7, and 14 days were washed with pre-cooled PBS. They were digested with 0.25% EDTA-free trypsin (Catalog no. 15090-046, Gibco) and centrifuged at 1000 rpm for 5 min. Cells were then placed in 1× binding buffer, collected by centrifugation again, and 10 µl of Annexin V-FITC stain and 10 µl of PI stain were added, respectively. After avoiding light for 10 min, the apoptosis rate was detected by flow cytometry (BD FACSARIA II, BD Biosciences). The sum of early apoptosis (Annexin V-FITC positive, PI negative) and late apoptosis (Annexin V-FITC positive, PI positive) was the apoptosis rate.

Alkaline phosphatase activity (ALP)

The spectrophotometric method was employed to ascertain ALP activity. Specifically, hBMSCs were seeded into 96-well plates at a density of 5×10^3 cells/well. After a 24-hour incubation period, the PM was substituted with OM. Following 7 consecutive days of incubation, the supernatant was harvested, and the level of ALP activity was quantified utilizing the commercial ALP assay kit (catalog no. CS0740, Sigma-Aldrich).

Separation of cytoplasm and nucleus

Subcellular localization analysis using the PARIS kit (catalog no. AM1921, Life Technologies). hBMSCs were harvested and subsequently washed using pre-chilled PBS. Following this, a cytoplasmic extraction buffer was introduced, and the cells underwent incubation on ice for 10 min, accompanied by vigorous agitation. This was followed by centrifugation at a speed of 12,000 rpm. The supernatant was subsequently moved to a newly pre-cooled tube for isolating the cytoplasmic extract. Meanwhile, the precipitate underwent further lysis with cytosolic lysis buffer for 60 s. Following this, cytosolic extracts were harvested through centrifugation at 14,000 rpm and maintained at 4°C. The abundance of LINC00968 mRNA in both the cytoplasm and nucleus was quantified using RT-qPCR, employing GAPDH as the cytoplasmic endogenous control and U6 as the nuclear endogenous control.

Bioinformatics analysis

LncRNASNP2 database (<https://guolab.wchscu.cn/lncRNASNP/#/>) predicts target miRNAs for LINC00968. Target mRNAs for miR-17-5p were predicted using ENCORI (<https://rnasysu.com/encori/index.php>), Tar

getscan (https://www.targetscan.org/vert_72/), miRDB (<http://mirdb.org/miRDB/>), Tarbase ([https://dianalab-ce.uth.gr/tarbasev8](https://dianalab.ce.uth.gr/tarbasev8)), mirDIP (<http://ophid.utoronto.ca/mirDIP/>), and microT_CDS (<http://diana.imis.athena-innovation.gr/DianaTools/>) databases. Overlapping target genes from different databases were subsequently analyzed by Venn analysis (<http://bioinformatics.psb.ugent.be/webtools/Venn/>). The Toxicological Genome Database (CTD) database (<http://ctdbase.org/>) and GeneCard database (<https://www.genecards.org/>) were used to download OP-related target mRNAs. Venn analysis was also performed between OP-related target genes and predicted miR-17-5p targets to find OP-related target genes in the target mRNA of miR-17-5p. Their genes are then entered into a STRING database (<https://string-db.org/cgi/input.pl>) to generate a protein-protein interaction (PPI) network. Next, to obtain the hub genes, the degree of connectivity in the PPI network was analyzed by Cytoscape software (version 3.6.0).

Dual luciferase reporter (DLR) assay

LINC00968 and STAT3 sequences containing miR-17-5p binding sequences were subcloned into the luciferase reporter plasmid vector pmirGLO to obtain LINC00968-wild type (WT), STAT3-WT, LINC00968-mutant (MT), STAT3-WT recombinant luciferase reporter plasmid. The hBMSCs (1×10^5 cells/well) were inoculated into 24-well plates and the above recombinant plasmids were transfected with 50 nM inhibitor NC or miR-17-5 inhibitor under 5 µl Lipofectamine 3000 (catalog no. L3000015, Invitrogen), respectively. Cells were lysed after 48 h and relative luciferase activity was assessed by the dual luciferase reporter gene assay kit (catalog no. RG027, Beyotime Biotechnology).

Ago RNA Immunoprecipitation (RIP) assay

hBMSCs (2×10^5 cells/well) were inoculated into 6-well plates, transfected with different plasmids or oligonucleotides, and cultured for 7 d in OM. The cells were subsequently lysed in 1 ml RIP buffer followed by centrifugation at 12,000 g for 15 min. 100 µl of cell lysates were treated with Anti-ago2 antibody (dilution, 1:5000; catalog no. ab57116, Abcam) and negative control Anti-IgG (dilution, 1:5000; catalog no.03-110, Millipore)-coupled magnetic beads. The immunoprecipitated RNA was purified and subsequently reverse transcribed to cDNA and subjected to RT-qPCR reaction.

Statistical analysis

Statistical analysis and data visualization via SPSS and GraphPad Prism 9.0 were performed after collecting at least 3 replicates. All data were from three independent biological replicates each involving two technical replicates, and presented as mean ± SD. Differences between

the groups were examined using Student's t-test or ANOVA assay followed by Tukey's test. The receiver operating characteristic (ROC) curves were conducted to determine the accuracy of diagnosis. P less than 0.05 is considered statistically different.

Results

LINC00968 was sharply decreased in bone tissue and serum from patients with OP

The expression of LINC00968 in patients with OP was first analyzed. As illustrated in Fig. 1A, a notable down-regulation of LINC00968 expression is observed in the bone tissue of OP patients compared to the controls ($P < 0.0001$). Consistently, a similar pattern was observed in the serum, showing a noticeable reduction

in LINC00968 levels in patients with OP ($P < 0.0001$, Fig. 1B). Furthermore, a significant positive correlation was observed between bone tissue and serum LINC00968 levels among OP patients ($r = 0.622$, $P < 0.001$, Fig. 1C). The ROC assay revealed that LINC00968 exhibited promising diagnostic significance, characterized by a sensitivity of 78.65% and a specificity of 71.95%, respectively, for differentiating controls from patients with OP (AUC = 0.800, 95%CI: 0.732–0.869, Fig. 1D).

Induction of osteogenic differentiation in hBMSCs attenuates apoptosis and enhances LINC00968 expression

We then established an osteogenic differentiation model using hBMSCs in vivo. Figure 2A demonstrates that these cells expressed CD29, CD44, CD73, and CD105

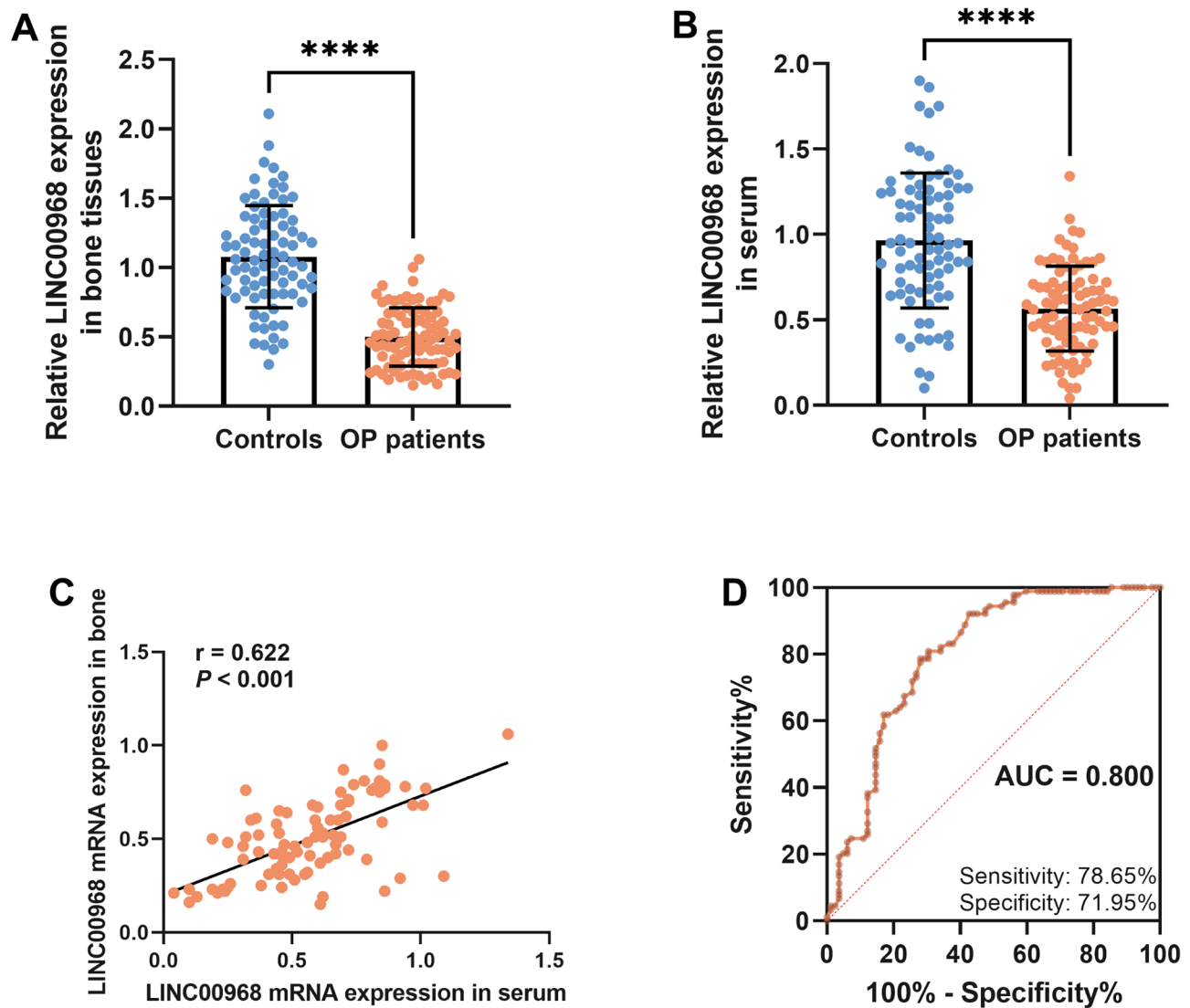


Fig. 1 The expression of LINC00968 in the patients with OP. **A.** The bone tissue of LINC00968 in the subjects was examined. **B.** The serum LINC00968 in the subjects was explored by the RT-qPCR assay. **C.** Pearson coefficient correlation was conducted to assess the correlation of serum LINC00968 and tissue LINC00968 in the patients with OP. **D.** Potential diagnostic significance of ROC curve test LINC00968 in identifying patients with OP. **** $P < 0.0001$

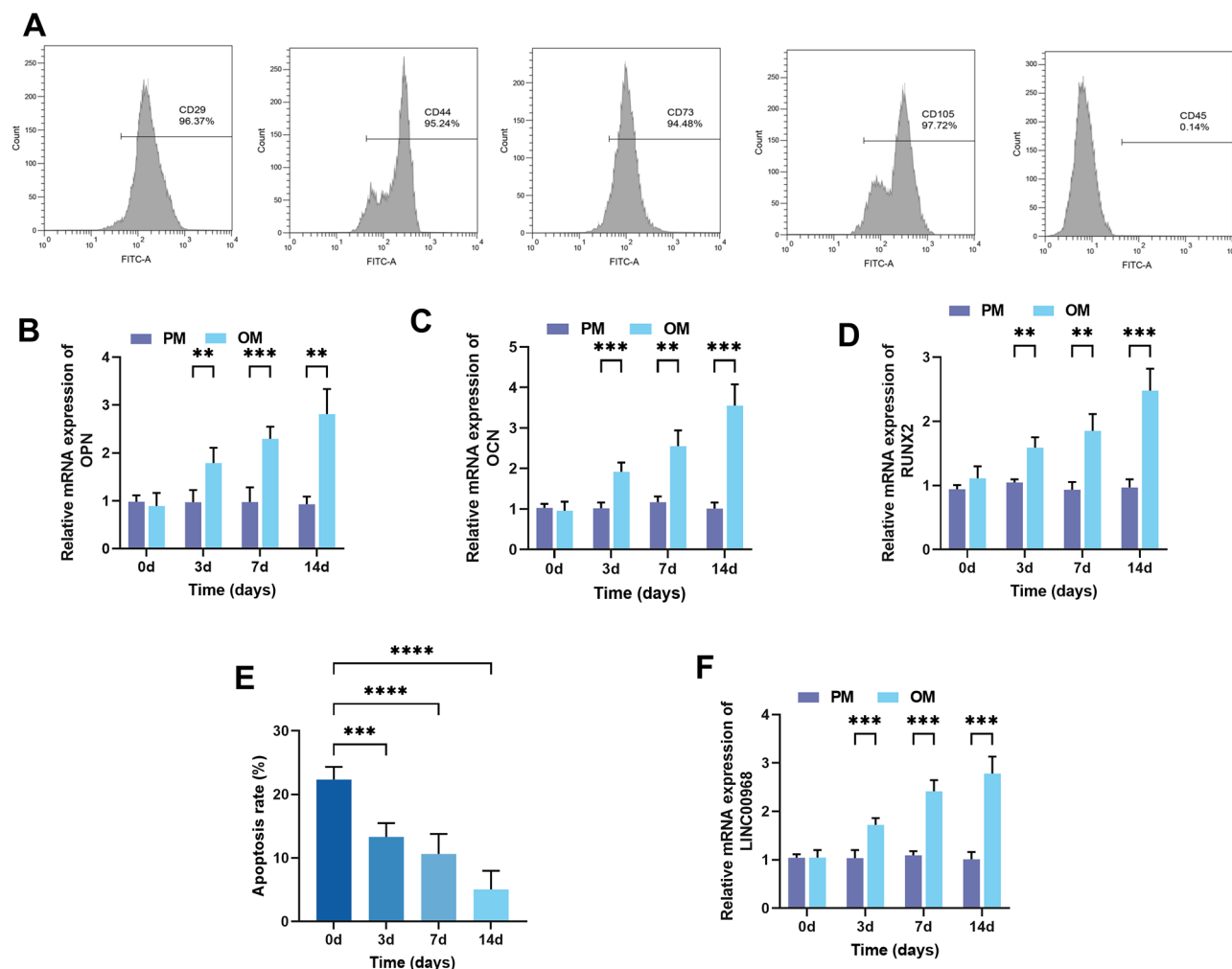


Fig. 2 Expression of LINC00968 in OM-induced osteogenic differentiation. **A.** Flow cytometry analysis of hBMSCs expression of cell surface markers. **B-D.** The expression of osteogenic differentiation markers of OPN, OCN, and RUNX2 with increasing OM induction time. **E.** Effect of osteogenic differentiation induction on apoptosis of hBMSCs with increasing OM induction time. **F.** RT-qPCR assay to detect the effect on LINC00968 mRNA levels with increasing OM induction time. ** $P < 0.01$, *** $P < 0.001$, **** $P < 0.0001$

positively, but CD45 negatively. As shown in Fig. 2B-D, the mRNA expression of OPN, OCN, and RUNX2 progressively increased with time during the osteogenic differentiation process induced by OM ($P < 0.001$). Furthermore, the apoptosis of hBMSCs gradually decreased with increasing OM induction time ($P < 0.001$, Fig. 2E). It is noteworthy that the mRNA level of LINC00968 increased gradually with the extension of OM induction time than the PM ($P < 0.005$, Fig. 2F).

Silencing of LINC00968 inhibits osteogenic differentiation and promotes apoptosis in hBMSCs

To further analyze the role of LINC00968 in osteogenic differentiation, the expression of LINC00968 in hBMSCs was artificially reduced. As depicted in Fig. 3A, transfection with si-LINC00968 notably diminished the level of LINC00968 compared to si-NC ($P < 0.0001$). Among the siRNA plasmids, si-LINC00968 #2 exhibited the highest

efficacy in downregulating LINC00968 mRNA, prompting its selection for use in all subsequent investigations. Furthermore, the promoting effect of OM on LINC00968 in hBMSCs was significantly attenuated by si-LINC00968 ($P < 0.0001$, Fig. 3B). In addition, si-LINC00968 typically suppressed the increase of ALP activity in hBMSCs by OM ($P < 0.0001$, Fig. 3C). Notably, OM induction distinctly upregulated the mRNA and protein expression of OPN, OCN, and RUNX2, whereas si-LINC00968 significantly downregulated their expression ($P < 0.001$, Fig. 3D-E and Supplemental Figure S1). Additionally, OM persistently suppressed apoptosis compared to the PM; however, the introduction of si-LINC00968 partially reversed the apoptosis rate ($P < 0.001$, Fig. 3F).

LINC00968 interacts with miR-17-5p

Subcellular localization analysis revealed that LINC00968 is predominantly located in the cytoplasm (Fig. 4A),

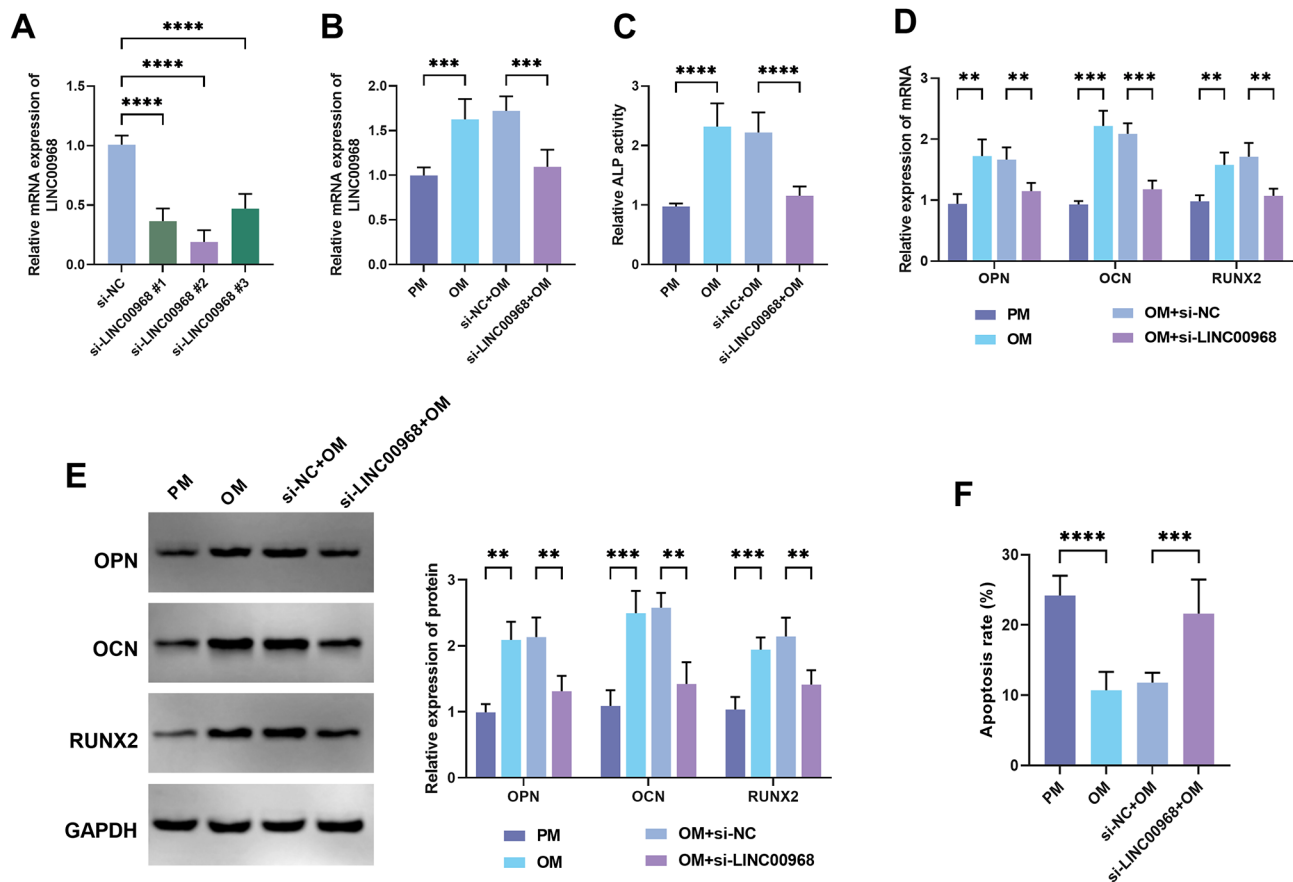


Fig. 3 Silencing of LINC00968 inhibits osteogenic differentiation and promotes apoptosis in hBMSCs. **A.** Inhibitory effect of transfection of si-LINC00968 on LINC00968 levels in hBMSCs. **B.** Quantitative analysis of LINC00968 levels in hBMSCs transfected with si-LINC00968 and induced for 3 days by OM. **C.** The ALP activity of inhibiting LINC00968 in the hBMSCs under OM was induced for 7 days. **D-E.** The mRNA and protein expression levels of OPN, OCN, and RUNX2 in hBMSCs were assessed after treatment with si-LINC00968 and OM for 3 days. **F.** The apoptosis rate of hBMSCs after transfection si-LINC00968 induced by OM for 3 days. ** $P < 0.01$, *** $P < 0.001$, **** $P < 0.0001$

suggesting that it has the potential to act as a molecular sponge for lncRNAs. Database predictions revealed that LINC00968 has a target binding site to miR-17-5p, and the putative binding sequence is presented in Fig. 4B. Furthermore, the miR-17-5p inhibitor can reduce the luciferase of LINC00968-WT than the inhibitor NC ($P < 0.001$) but has no function in the LINC00968-MT ($P > 0.05$, Fig. 4C). Moreover, compared with the anti-IgG, miR-17-5p and LINC00968 were all enriched in the anti-Ago group ($P < 0.0001$, Fig. 4D). In bone tissues and serum samples, miR-17-5p levels were higher in OP patients than in controls ($P < 0.0001$, Fig. 4E-F). In OP patients, bone tissue miR-17-5p was negatively correlated with LINC00968 ($r = -0.736$, $P < 0.001$, Fig. 4G), while serum miR-17-5p was also negatively correlated with serum LINC00968 ($r = -0.771$, $P < 0.001$, Fig. 4H). Moreover, miR-17-5p levels progressively decreased over time in OM-induced hBMSCs ($P < 0.0001$, Fig. 4I). Furthermore, the reduction in miR-17-5p levels caused by OM induction was noticeably reversed by the introduction of si-LINC00968 ($P < 0.001$, Fig. 4J).

Inhibition of miR-17-5p reverses the functions of si-LINC00968 on OM-induced osteogenic differentiation and apoptosis

The miR-17-5p inhibitor significantly reduced miR-17-5p compared to the inhibitor NC ($P < 0.005$, Fig. 5A). Meanwhile, the promoting effect of si-LINC00968 on the level of miR-17-5p induced by OM was significantly weakened by miR-17-5p inhibitor ($P < 0.001$, Fig. 5B). Intriguingly, the reduction in ALP activity induced by si-LINC00968 was subsequently and notably rescued by miR-17-5p inhibitor under the OM induction ($P < 0.001$, Fig. 5C). Furthermore, the mRNA and protein expression of OPN, OCN, and RUNX2 were diminished by the si-LINC00968, while this suppression was partially alleviated following the administration of a miR-17-5p inhibitor ($P < 0.001$, Fig. 5D-E and Supplemental Figure S2). Additionally, si-LINC00968 distinctly enhanced OM-induced apoptosis in hBMSCs, but this enhancement was typically diminished by miR-17-5p inhibitor ($P < 0.001$, Fig. 5F).

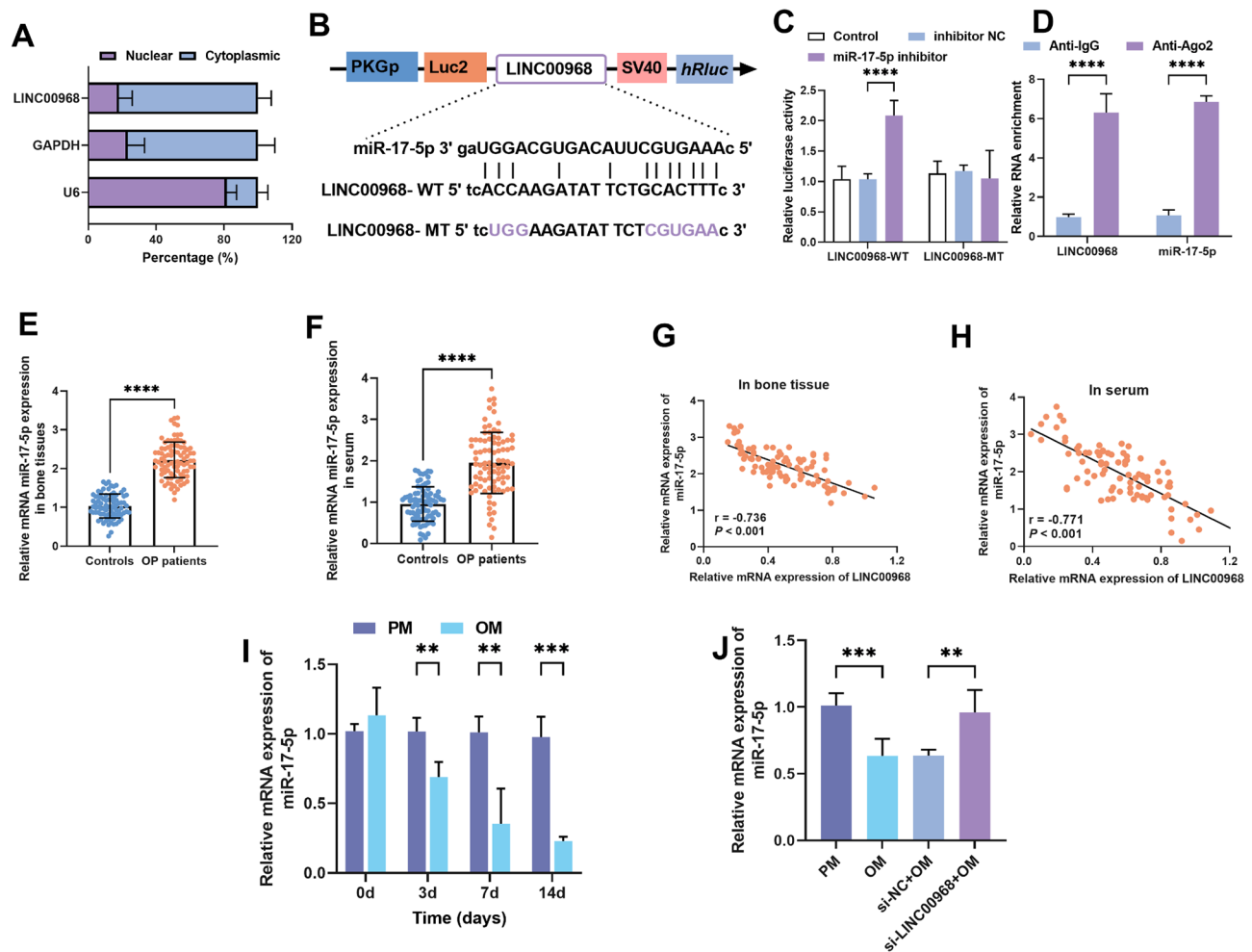


Fig. 4 LINC00968 interacts with miR-17-5p. **A**. The subcellular location analysis of the LINC00968 in the hBMSCs. **B**. The putative binding sequences between LINC00968 and miR-17-5p. **C-D**. The dual luciferase reporter assay and RIP assay were conducted to examine the relationship between LINC00968 and miR-17-5p. **E-F**. The levels of miR-17-5p in the bone tissue and serum of patients with OP were examined. **G-H**. The Spearman coefficient correlation examined the relationship between LINC00968 and miR-17-5p in the bone tissues and serum samples. **I**. Changes in miR-17-5p expression in hBMSCs with increasing OM induction time. **J**. Effect of OM-induced and transfected si-LINC00968 on miR-17-5p levels in hBMSCs. ** $P < 0.01$, *** $P < 0.001$, **** $P < 0.0001$

STAT3 is targeted by miR-17-5p

An extensive search across six databases yielded 166 common targets for miR-17-5p (Fig. 6A). Among these, 52 targets were found to be associated with OP (Fig. 6B). A PPI network was constructed, encompassing 52 nodes connected by 52 edges with an enrichment P-value below $1.05e-0.7$ (Fig. 6C). The top 10 genes ranked the connectivity degree, were HIF1A, STAT3, CDKN1A, E2F1, MAP3K5, TGFBR2, HMAG2, RBBP7, TSG101, and TXNIP (Supplemental Figure S3). Given STAT3's crucial role in OP and multiple reports of miR-17-5p targeting STAT3, we focused on STAT3 in our studies. The putative binding site of STAT3 for miR-17-5p is depicted in Fig. 6D. Furthermore, miR-17-5p inhibitor could suppress the luciferase of STAT3-WT but did not affect STAT3-MT compared to inhibitor NC ($P > 0.05$, Fig. 6E). Furthermore, miR-17-5p, LINC00968, and STAT3 were

all enriched in the Anti-ago2 ($P < 0.0001$, Fig. 6F). Both bone tissue and serum STAT3 levels were generally lower in OP patients than in controls ($P < 0.0001$, Fig. 6G-H). Serum STAT3 was positively associated with serum LINC00968 levels ($r = 0.612$, $P < 0.0001$, Fig. 6I) and negatively associated with serum miR-17-5p expression ($r = -0.619$, $P < 0.0001$, Fig. 6J), respectively. Moreover, STAT3 expression was elevated in hBMSCs with increasing OM induction time ($P < 0.001$, Fig. 6K). si-LINC00968 suppressed STAT3 expression in OM-induced hBMSCs, however, this suppression was abolished by miR-17-5p inhibitor ($P < 0.001$, Fig. 6L).

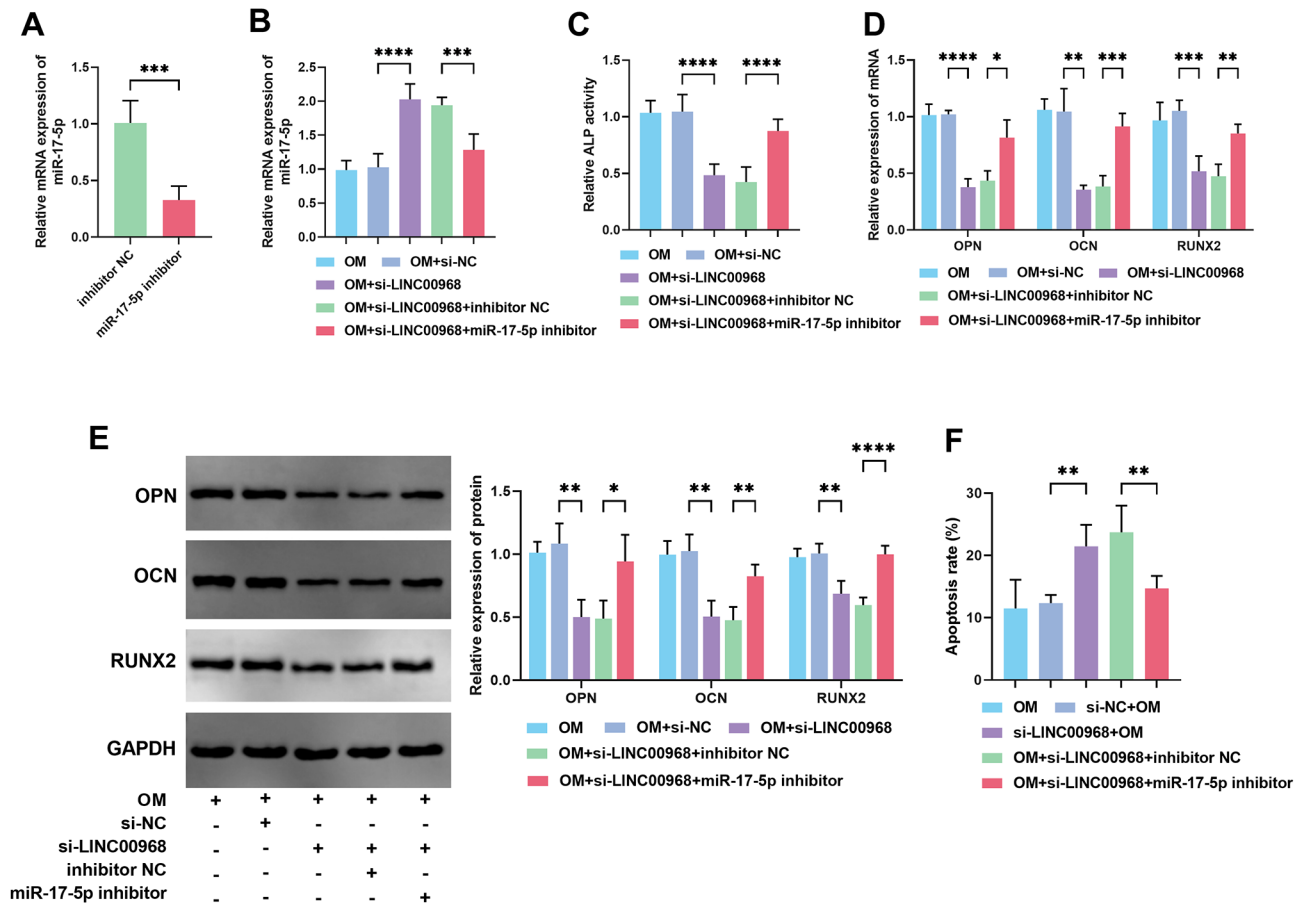


Fig. 5 LINC00968 modulates the osteogenic differentiation and apoptosis in hBMSCs through the targeting of miR-17-5p. **A-B.** The levels of miR-17-5p were assessed following standalone transfection with miR-17-5p inhibitor or in the presence of OM induction for 3 days, as well as during co-transfection with si-LINC00968. **C.** The ALP activity at 7 days of OM induction was co-regulated by si-LINC00968 and miR-17-5p inhibitor. **D-E.** The mRNA and protein levels of osteogenic differentiation markers were co-regulated by si-LINC00968 and a miR-17-5p inhibitor after 3 days of OM induction. **F.** Apoptosis rate of cells at 3 days of OM induction and co-transfected with si-LINC00968 and miR-17-5p inhibitor detected by flow cytometry. ** $P < 0.01$, *** $P < 0.001$, **** $P < 0.0001$

Discussion

OP is a systemic skeletal disorder caused by impaired function of endogenous BMSCs leading to increased fracture risk. OP often goes unnoticed due to its asymptomatic nature, typically coming to medical attention only after the occurrence of the first fracture. Conversely, treatments such as bisphosphonates and intermittent parathyroid hormone, which serve to inhibit bone resorption and stimulate bone formation, are not only accompanied by adverse effects but also result in suboptimal therapeutic outcomes [22]. For example, although small doses of parathyroid hormone (PTH) promote bone formation, it is expensive, inconvenient to inject, ineffective, and is not yet widely used [23]. Hence, timely diagnosis, novel therapeutic strategies, and preventive interventions are crucial for managing OP. The osteogenic differentiation potential of BMSCs in tendon, cartilage, and bone regeneration is widely recognized [24]. Diminished differentiation can hinder bone formation

and expedite OP progression. Consequently, researchers are actively pursuing various approaches to enhance BMSCs' osteogenic differentiation to slow OP progression, including exogenous magnetic fields [25] and ncRNA regulation [26–28]. Notably, lncRNAs play a pivotal role in osteogenesis and serve as potential clinical biomarkers, garnering significant interest from the research community. For example, lncRNA GAS5 as a diagnostic biomarker remarkably differentiates patients with OP from healthy controls [29]. Plasma lncRNA MALAT1 expression is negatively correlated with the severity of postmenopausal osteoporosis patients and has a good diagnostic value for the degree of fracture [30]. Therefore, identifying lncRNAs that regulate osteogenic differentiation is crucial for diagnosing and managing OP patients.

As a novel lncRNA, LINC00968 has been found to have high sensitivity and specificity in distinguishing breast cancer patients from healthy individuals [31],

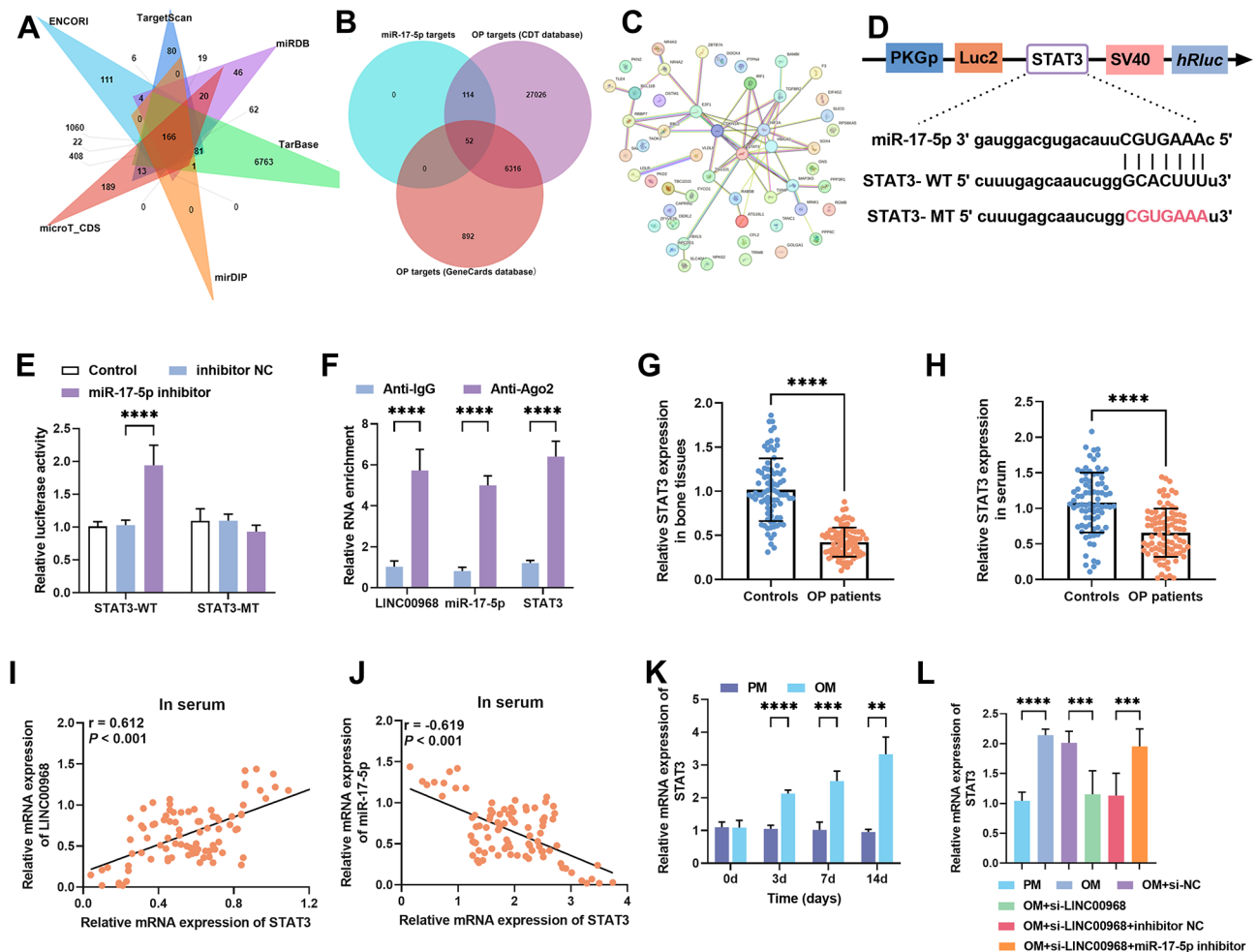


Fig. 6 STAT3 is targeted by miR-17-5p. **A**. The target of miR-17-5p was predicted by the starbases. **B**. Venn diagram displayed the overlapping targets of miR-17-5p and OP-related targets. **C**. The overlapping targets were examined by the PPI network, and the top 5 hub genes were identified. **D**. The putative binding site of STAT3 for miR-17-5p. **E-F**. The dual luciferase reporter assay and RIP assay were conducted to examine the relationship between STAT3 and miR-17-5p. **G-H**. The levels of STAT3 in the bone tissue and serum of patients with OP were examined. **I-J**. The Spearman coefficient correlation examined the relationship between serum miR-17-5p with serum STAT3 or serum LINC00968. **K**. Changes in STAT3 expression in hBMSCs with increasing OM induction time. **L**. Effect of OM-induced and transfected si-LINC00968 and miR-17-5p inhibitor on STAT3 levels in hBMSCs. ** $P < 0.01$, *** $P < 0.001$, **** $P < 0.0001$

suggesting its potential as a clinical biomarker. In bone-related diseases, specifically osteosarcoma progression, LINC00968 is involved in regulating migration and invasion [7]. Furthermore, prior research has demonstrated that LINC00968 modulates the osteogenic differentiation of dental pulp stem cells in vitro, as well as bone formation in vivo [8]. Additionally, the expression of glucagon-like peptide 1 receptor by osteoblasts enhances bone formation during zebrafish scale regeneration, a process that involves the regulation of LINC00968 [9]. In 2017, Qiu et al. conducted a microarray analysis to investigate aberrantly expressed long non-coding RNAs (lncRNAs) during the osteogenic differentiation of human bone marrow mesenchymal stem cells. Among the identified lncRNAs, LINC00968 exhibited a statistically significant difference with a fold change greater than 2 [10]. However, the expression pattern of LINC00968 in OP and its

regulatory mechanisms within hBMSCs remain poorly characterized. Our study is the first to demonstrate a significant downregulation of LINC00968 in both the serum and bone tissue samples from patients with OP. Furthermore, serum LINC00968 levels exhibit high diagnostic potential, effectively distinguishing OP patients from controls. Meanwhile, Consistent with our previous findings, abnormal expression of LINC00968 was also observed during osteogenic differentiation, but inhibition of LINC00968 prevented the formation of biomarkers of bone formation and promoted apoptosis in hBMSCs. The results suggest that osteogenic differentiation can be promoted by promoting LINC00968 expression, which promotes bone formation and contributes to bone repair in OP.

Molecularly, lncRNAs located in the cytoplasm can act as molecular sponges for miRNAs and inhibit their

expression, thereby positively regulating mRNA levels [32]. We found in this study that LINC00968 was mainly enriched in the cytoplasm, therefore we tried to identify its potential downstream miRNAs. miR-17-5p levels were notably increased in patients with postmenopausal OP [17]. Furthermore, miR-17-5p serves as an inducer of diminished bone mineral density in the OP mice model induced by ovariectomy [16]. Consistent with their results, we also found that miR-17-5p was significantly elevated in both bone tissue and serum of patients with OP. However, we demonstrated for the first time that the expression of LINC00968 was negatively correlated with miR-17-5p. The role of miR-17-5p in the bone differentiation of hBMSCs has also been identified. Liu et al. (2022), through sequencing analysis, identified a significant reduction in miR-17-5p levels among differentially expressed lncRNAs in rat BMSCs at 14 days of osteogenic differentiation [33]. miR-17-5p inhibits osteogenic differentiation of mouse embryonic osteoblast precursor cells MC3T3-E1 [34]. During vascular calcification, the overexpression of miR-17-5p via lipid nanoparticles inhibited the expression of osteogenic gene RUNX2, inhibited calcium deposition in vascular smooth muscle cells, and suppressed their osteogenic differentiation [35]. In line with these observations, we also discovered that miR-17-5p levels were significantly decreased during osteogenic differentiation of hBMSCs. However, for the first time, we discovered that the inhibition of osteogenic differentiation of hBMSCs caused by silencing LINC00968 was significantly reversed by low expression of miR-17-5p, and apoptosis was attenuated. In conclusion, LINC00968 may have promoted hBMSCs osteogenic differentiation by targeting miR-17-5p.

STAT3 plays a pivotal function including cell differentiation, apoptosis, and angiogenesis [36]. Previous studies have reported that STAT3 is critical for skeletal development and femoral homeostasis and has emerged as a key target for mitigating OP progression [37]. For instance, naringenin enhances bone formation and facilitates the progression of OP via the modulation of STAT3 [20]. Additionally, puerarin has demonstrated efficacy in mitigating OP in rats by specifically targeting STAT3 [38]. Furthermore, catalpol stimulates the coupling of osteogenesis and angiogenesis in BMSCs through the activation of STAT3, ultimately expediting bone repair processes in individuals with OP [19]. STAT3 knockout mice had shortened limbs, multiple fractures of long bones, reduced cortical bone thickness and bone volume, and suppressed osteogenic differentiation of BMSCs *in vitro* [21]. Consistent with previous studies, we found that STAT3 levels were typically reduced in bone tissue and serum from patients with OP and significantly elevated during osteogenic differentiation of hBMSCs induced by OM. Previous studies have reported miR-17-5p targeting

STAT3 in rheumatoid arthritis [33], bladder cancer [39], and myocardial ischemia-reperfusion injury [40]. In line with prior research, our study pinpointed STAT3 as a direct target gene of miR-17-5p in the context of OP. However, our investigation revealed a novel finding: a negative correlation between STAT3 expression and miR-17-5p levels, alongside a positive association with LINC00968 abundance in OP patients. Additionally, we observed that the upregulation of STAT3 induced by OM was markedly mitigated upon LINC00968 downregulation, whereas this attenuation was substantially reversed when miR-17-5p was inhibited.

Although LINC00968's role in dental pulp stem cell osteogenic differentiation is known, our study focused on its unique role in OP. As a complex disease, OP differs markedly from normal osteogenic differentiation. Thus, LINC00968's specific mechanisms, regulatory networks, and clinical applications in OP were unexplored. Our study confirmed LINC00968's regulation in osteoporotic osteoblast differentiation and explored its molecular mechanisms, including miR-17-5p/STAT3 interactions, providing clues for understanding OP and developing new treatments. The decreased expression level of LINC00968 in OP patients suggests that it may be a promising diagnostic biomarker, and its decreased expression level may be predictive of OP, providing clues for clinicians to recognize patients early, thus contributing to the early diagnosis of OP. In addition, given the promotional effect of LINC00968 or the design of specific inhibitors targeting the miR-17-5p/STAT3 axis could potentially promotionally promote bone formation and alleviate the progression of OP.

Limitations of this study affect its applicability. Although protein and RNA levels of osteogenic markers OCN, OPN, RUNX2, and ALP activity were analyzed, alizarin red staining is required for further confirmation. In addition, both cell generation and status may affect mRNA levels of osteogenic markers, but we added more stable protein expression for further confirmation. Furthermore, although previous studies reported the role of the EGF signaling pathway and TGF β signaling pathway in osteogenesis [41, 42], whether the LINC00968/miR-17-5p/STAT3 axis affects them needs further confirmation. What's more, we employed standardized hBMSCs from ATCC to ensure consistency and reliability. Nevertheless, BMSCs derived from healthy individuals and OP patients may exhibit variations in LINC00968 expression, potentially influenced by genetic background, environmental factors, and disease status. Future research will delve into these differences to offer novel insights into OP and potential treatments. Moreover, while this study initially showed LINC00968 and miR-17-5p regulate OP progression, their clinical use is limited by complex *in vivo* mechanisms, off-target effects, drug delivery

challenges, individual variations, and long-term safety and efficacy concerns that require further investigation.

Conclusions

Herein, we discerned diminished expression of LINC00968 in patients with OP, underscoring its utility as a promising diagnostic biomarker. Furthermore, LINC00968 can regulate the miR-17-5p/STAT3 axis, thereby enhancing osteoblastic differentiation of hBMSCs and repressing apoptosis. This mechanism may represent a novel therapeutic approach for bone repair in OP and provide fresh perspectives for future investigations into osteogenic differentiation and the management of OP.

Abbreviations

ALP	Alkaline phosphatase activity
BMSCs	Bone marrow mesenchymal stem cells
cDNA	Complementary DNA
DLR	Dual luciferase reporter
hBMSCs	Human BMSCs
LINC00968	Long intergenic non-protein coding RNA 968
LncRNAs	Long non-coding RNAs
MT	Mutant
NC	Negative control
OCN	Osteocalcin
OM	Osteogenic differentiation medium
OP	Osteoporotic
OPN	Osteopontin
PM	Proliferation medium
PPI	Protein-protein interaction
RIP	RNA Immunoprecipitation
ROC	Receiver operating characteristic
RT-qPCR	Real-time quantitative reverse transcription PCR
RUNX2	Runt-related transcription factor 2
si-LINC00968	Small interfering RNA targeting LINC00968
STAT3	Signal transducer and activator of transcription 3
WT	Wild type

Supplementary Information

The online version contains supplementary material available at <https://doi.org/10.1186/s13018-025-05627-0>.

Supplementary Material 1

Acknowledgements

Not applicable.

Author contributions

All authors designed this study. SL N, Y C and H Z conducted the experiment and analyzed the data. SL N wrote the manuscript. H Z revised the manuscript. All authors reviewed and approved for publication.

Funding

The study was funded by China postdoctoral science foundation grant (No: 2018M641663).

Data availability

The datasets used and/or analysed during the current study are available from the corresponding author on reasonable request.

Declarations

Ethics approval and consent to participate

The study was approved by the Tianjin Hospital Research Ethics Committee. The experimental procedures were under the standards fixed in the Declaration of Helsinki, and the subjects were informed about the research design and signed an informed consent form.

Consent for publication

Not applicable.

Competing interests

The authors declare no competing interests.

Received: 1 November 2024 / Accepted: 18 February 2025

Published online: 06 March 2025

References

- Li M, Tang Q, Liao C, Wang Z, Zhang S, Liang Q, et al. Extracellular vesicles from apoptotic BMSCs ameliorate osteoporosis via transporting regenerative signals. *Theranostics*. 2024;14(9):3583–602.
- Li T, Yuan J, Xu P, Jia J, Zhao J, Zhang J, et al. PMAIP1, a novel diagnostic and potential therapeutic biomarker in osteoporosis. *Aging*. 2024;16(4):3694–715.
- Huang C, Wang Y. Downregulation of METTL14 improves postmenopausal osteoporosis via IGF2BP1 dependent posttranscriptional silencing of SMAD1. *Cell Death Dis*. 2022;13(11):919.
- Qin S, Liu D. Long non-coding RNA H19 mediates osteogenic differentiation of bone marrow mesenchymal stem cells through the miR-29b-3p/DKK1 axis. *J Cell Mol Med*. 2024;28(9):e18287.
- Wumiti T, Wang L, Xu B, Ma Y, Zhu Y, Zuo X, et al. lncTIMP3 promotes osteogenic differentiation of bone marrow mesenchymal stem cells via miR-214/Smad4 axis to relieve postmenopausal osteoporosis. *Mol Biol Rep*. 2024;51(1):719.
- Tang JZ, Zhao GY, Zhao JZ, Di DH, Wang B. LncRNA IGF2-AS promotes the osteogenic differentiation of bone marrow mesenchymal stem cells by sponging miR-3,126-5p to upregulate KLK4. *J Gene Med*. 2021;23(10):e3372.
- Liu G, Yuan D, Sun P, Liu W, Wu PF, Liu H, et al. LINC00968 functions as an oncogene in osteosarcoma by activating the PI3K/AKT/mTOR signaling. *J Cell Physiol*. 2018;233(11):8639–47.
- Liao C, Zhou Y, Li M, Xia Y, Peng W. LINC00968 promotes osteogenic differentiation in vitro and bone formation in vivo via regulation of miR-3658/RUNX2. *Differentiation*. 2020;116:1–8.
- Zhai S, Liu C, Vimalraj S, Subramanian R, Abullais SS, Arora S, et al. Glucagon-like peptide-1 receptor promotes osteoblast differentiation of dental pulp stem cells and bone formation in a zebrafish scale regeneration model. *Peptides*. 2023;163:170974.
- Qiu X, Jia B, Sun X, Hu W, Chu H, Xu S, et al. The critical role of long noncoding RNA in osteogenic differentiation of human bone marrow mesenchymal stem cells. *Biomed Res Int*. 2017;2017:5045827.
- Giordano L, Porta GD, Peretti GM, Maffulli N. Therapeutic potential of MicroRNA in tendon injuries. *Br Med Bull*. 2020;133(1):79–94.
- Oliviero A, Della Porta G, Peretti GM, Maffulli N. MicroRNA in osteoarthritis: pathophysiology, diagnosis and therapeutic challenge. *Br Med Bull*. 2019;130(1):137–47.
- Gargano G, Oliviero A, Oliva F, Maffulli N. Small interfering RNAs in tendon homeostasis. *Br Med Bull*. 2021;138(1):58–67.
- Gargano G, Oliva F, Oliviero A, Maffulli N. Small interfering RNAs in the management of human rheumatoid arthritis. *Br Med Bull*. 2022;142(1):34–43.
- Gargano G, Asparago G, Spiezia F, Oliva F, Maffulli N. Small interfering RNAs in the management of human osteoporosis. *Br Med Bull*. 2023;148(1):58–69.
- Hao L, Li J, Tian Y, Wu J. Changes in the MicroRNA profile of the mandible of ovariectomized mice. *Cell Physiol Biochem*. 2016;38(4):1267–87.
- Wang R, Lu A, Liu W, Yue J, Sun Q, Chen J, et al. Searching for valuable differentially expressed miRNAs in postmenopausal osteoporosis by RNA sequencing. *J Obstet Gynaecol Res*. 2020;46(7):1183–92.
- Sobah ML, Liongue C, Ward AC. Contribution of signal transducer and activator of transcription 3 (STAT3) to bone development and repair. *Int J Mol Sci*. 2023;25(1):389.

19. Chen L, Zhang RY, Xie J, Yang JY, Fang KH, Hong CX, et al. STAT3 activation by Catalpol promotes osteogenesis-angiogenesis coupling, thus accelerating osteoporotic bone repair. *Stem Cell Res Ther*. 2021;12(1):108.
20. Wang W, Mao J, Chen Y, Zuo J, Chen L, Li Y, et al. Naringin promotes osteogenesis and ameliorates osteoporosis development by targeting JAK2/STAT3 signalling. *Clin Exp Pharmacol Physiol*. 2022;49(1):113–21.
21. Huang Z, Feng J, Feng X, Chan L, Lu J, Lei L, et al. Loss of signal transducer and activator of transcription 3 impaired the osteogenesis of mesenchymal progenitor cells in vivo and in vitro. *Cell Biosci*. 2021;11(1):172.
22. Xue J, Liu L, Liu H, Li Z. LncRNA SNHG14 activates autophagy via regulating miR-493-5p/Mef2c axis to alleviate osteoporosis progression. *Commun Biol*. 2023;6(1):1120.
23. Che M, Gong W, Zhao Y, Liu M. Long noncoding RNA HCG18 inhibits the differentiation of human bone marrow-derived mesenchymal stem cells in osteoporosis by targeting miR-30a-5p/NOTCH1 axis. *Mol Med*. 2020;26(1):106.
24. Giai Via A, McCarthy MB, de Girolamo L, Ragni E, Oliva F, Maffulli N. Making them commit: strategies to influence phenotypic differentiation in mesenchymal stem cells. *Sports Med Arthrosc Rev*. 2018;26(2):64–9.
25. Barnaba S, Papalia R, Ruzzini L, Sgambato A, Maffulli N, Denaro V. Effect of pulsed electromagnetic fields on human osteoblast cultures. *Physiother Res Int*. 2013;18(2):109–14.
26. Liu L, Yang Y, Sun P. LINC00941 affects the proliferation, apoptosis and differentiation of osteoblasts by regulating the miR-335-5p/KAT7 axis. *J Orthop Surg Res*. 2025;20(1):75.
27. Hu Y, Cen M, Hu Y. Exploring the role of OIP5-AS1 in the mechanisms of delayed fracture healing: functional insights and clinical implications. *J Orthop Surg Res*. 2025;20(1):32.
28. Chen Q, Huang L, Ji W, Huang M, Sima J, Li J, et al. LINC01271 promotes fracture healing via regulating miR-19a-3p/PIK3CA axis. *J Orthop Surg Res*. 2025;20(1):33.
29. Cong C, Tian J, Gao T, Zhou C, Wang Y, Cui X, et al. LncRNA GASS is upregulated in osteoporosis and downregulates miR-21 to promote apoptosis of osteoclasts. *Clin Interv Aging*. 2020;15:1163–9.
30. Qian TY, Wan H, Huang CY, Hu XJ, Yao WF. Plasma LncRNA MALAT1 expressions are negatively associated with disease severity of postmenopausal osteoporosis. *Lab Med*. 2022;53(5):446–52.
31. Wang M, Liu H, Wu W, Zhao J, Song G, Chen X, et al. Identification of differentially expressed plasma LncRNAs as potential biomarkers for breast Cancer. *Clin Breast Cancer*. 2022;22(2):e135–41.
32. Yan Y, Wang J, Xu B, Ni J, Dai T, Wang L, et al. Exosomal SOX21-AS1 regulates EREG by sponging miR-451a and promotes the malignancy of pancreatic ductal adenocarcinoma. *J Cancer*. 2024;15(11):3321–37.
33. Duan B, Yu Z, Liu R, Li J, Song Z, Zhou Q, et al. Tetrandrine-induced down-regulation of LncRNA NEAT1 inhibits rheumatoid arthritis progression through the STAT3/miR-17-5p pathway. *Immunopharmacol Immunotoxicol*. 2022;44(6):886–93.
34. Fang T, Wu Q, Zhou L, Mu S, Fu Q. miR-106b-5p and miR-17-5p suppress osteogenic differentiation by targeting Smad5 and inhibit bone formation. *Exp Cell Res*. 2016;347(1):74–82.
35. Baba I, Matoba T, Katsuki S, Koga JI, Kawahara T, Kimura M, et al. EVs-miR-17-5p attenuates the osteogenic differentiation of vascular smooth muscle cells potentially via Inhibition of TGF-beta signaling under high glucose conditions. *Sci Rep*. 2024;14(1):16323.
36. Hou X, Tian F. STAT3-mediated osteogenesis and osteoclastogenesis in osteoporosis. *Cell Commun Signal*. 2022;20(1):112.
37. Zhou S, Dai Q, Huang X, Jin A, Yang Y, Gong X, et al. STAT3 is critical for skeletal development and bone homeostasis by regulating osteogenesis. *Nat Commun*. 2021;12(1):6891.
38. Zhao X, Zhou J, Liu Y, Wang J, Liu Y, Wang B, et al. Puerarin alleviates osteoporosis in rats by targeting the JAK2/STAT3 signaling pathway. *Biomol Biomed*. 2024;24(6):1651–61.
39. Xia Y, Chen S, Cui J, Wang Y, Liu X, Shen Y, et al. Berberine suppresses bladder cancer cell proliferation by inhibiting JAK1-STAT3 signaling via upregulation of miR-17-5p. *Biochem Pharmacol*. 2021;188:114575.
40. Chen J, Li X, Zhao F, Hu Y. HOTAIR/miR-17-5p Axis is involved in the Propofol-Mediated cardioprotection against ischemia/reperfusion injury. *Clin Interv Aging*. 2021;16:621–32.
41. Mangiavini L, Peretti GM, Canciani B, Maffulli N. Epidermal growth factor signalling pathway in endochondral ossification: an evidence-based narrative review. *Ann Med*. 2022;54(1):37–50.
42. Kay AG, Dale TP, Akram KM, Mohan P, Hampson K, Maffulli N, et al. BMP2 repression and optimized culture conditions promote human bone marrow-derived mesenchymal stem cell isolation. *Regen Med*. 2015;10(2):109–25.

Publisher's note

Springer Nature remains neutral with regard to jurisdictional claims in published maps and institutional affiliations.